PHYSICAL REVIEW B **77**, 020407(R) (2008)

Polaronic signature in the metallic phase of $La_{0.7}Ca_{0.3}MnO_3$ films detected by scanning tunneling spectroscopy

S. Seiro,* Y. Fasano, I. Maggio-Aprile, E. Koller, O. Kuffer, and Ø. Fischer
Département de Physique de la Matière Condensée, Université de Genève, 24, Quai Ernest-Ansermet, 1211 Geneva, Switzerland
(Received 23 July 2007; revised manuscript received 19 October 2007; published 18 January 2008)

In this work we map tunnel conductance curves with nanometric spatial resolution, tracking polaronic quasiparticle excitations when a $La_{0.7}Ca_{0.3}MnO_3$ film is cooled across the insulator-to-metal transition. In the insulating phase the spectral signature of polarons, a depletion of conductance at low bias flanked by peaks, is detected all over the scanned surface. These features are still observed at the transition and persist on cooling into the metallic phase. Polaron-binding-energy maps reveal that polarons are not confined to regions embedded in a highly conducting matrix but are present over the whole field of view both above and below the transition temperature.

DOI: 10.1103/PhysRevB.77.020407 PACS number(s): 75.47.Lx, 73.50.−h, 68.37.Ef, 71.30.+h

In manganite compounds such as $La_{1-x}Ca_xMnO_3$ ($0.2 < x < 0.5$), the coupling between lattice, magnetism, and transport leads to a transition from metallic ($d\rho/dT > 0$) to insulating ($d\rho/dT > 0$) behavior in tune with the suppression of ferromagnetic order at a temperature T_{MI}.[1,2] Understanding the transport properties of the insulating phase required the consideration of the electron-phonon coupling mechanism in addition to double-exchange interactions.[3,4] In the strong-coupling limit, electrons are bound by a surrounding lattice distortion forming polaronic quasiparticles.[3,4] In the insulating phase, polaron hopping is the dominant transport mechanism and gives rise to the measured thermally activated resistivity.[5–7] Theoretical predictions[3,4] state that on cooling below T_{MI} spin order leads to electron delocalization. In the case of the paradigmatic $La_{1-x}Ca_xMnO_x$ close to optimal doping, although some experimental data are consistent with a polaron collapse at T_{MI},[8–10] other reports provide evidence for the presence of polarons in the ferromagnetic metallic phase.[11–16] In this work we address this controversy by studying local electronic properties as a function of temperature on a single-crystalline fully strained $La_{0.7}Ca_{0.3}MnO_3$ film. Scanning tunneling spectroscopy (STS) was used to map the spatial dependence of polaronic spectral features over submicrometer regions.

The ability to probe electronic properties with spatial resolution at the microscopic scale makes STS a suitable technique to explore the possibility of electronic phase separation in manganites.[2] Although this scenario has gained popularity in recent years, it is mostly supported by results from macroscopic techniques.[2] Local spectroscopy studies in $La_{1-x}Ca_xMnO_3$ claim electronic phase separation,[17–20] but a strong influence of the chemical and structural disorder present in the samples cannot be ruled out. In contrast, a recent study in a fully relaxed film reports homogeneous conductance maps.[21] However, conductance maps at a fixed energy do not provide enough information on the eventual presence, spectroscopic characteristics, and spatial distribution of polaronic quasiparticles. Therefore, in this work we measure tunnel current vs voltage maps with nanometric spatial resolution in $La_{0.7}Ca_{0.3}MnO_3$ (LCMO) films, tracking polaronic quasiparticles when cooling across the metal-insulator transition (MIT). The spectral signature of polarons is observed both above and below T_{MI} all over the field of view.

The LCMO film studied in this work was grown on a $SrTiO_3$ substrate by rf sputtering at 675 °C, in 0.2 Torr of a 50% Ar–50% O_2 mixture. Great effort was made to obtain a single-crystalline fully strained film. By controlling strain, T_{MI} can be reduced with respect to the bulk[22] allowing access to a wider temperature range of the insulating phase. The structure of three-dimensional perovskites does not present an easy cleaving plane, so we thoroughly cleaned the surface of the film with isopropanol in an ultrasonic bath. The sample was immediately placed in the ultrahigh-vacuum chamber of a variable-temperature homemade STS system,[23] prior to cooling in ^{4}He exchange gas. This procedure allowed us to obtain reproducible and high-quality topographic images like the one shown in Fig. 1. Topographs and current vs voltage $[I(V)]$ maps were measured as a function of temperature, with particular detail in the range around T_{MI}. The tip, made of electrochemically etched Ir, was grounded and the bias voltage V was applied to the sample.

The thickness of the film, 31 nm, was obtained from x-ray reflectometry and confirmed by the Laue oscillations around the (002) reflection, which is shown in Fig. 1(a). The c axis parameter was found to be 3.808 ± 0.002 Å, 1.6% smaller than that of the bulk, as expected for tensile in-plane strain. The reciprocal space map in Fig. 1(b) shows that the in-plane lattice parameter matches that of $SrTiO_3$, i.e., the film is fully strained. The (103) pole figure in Fig. 1(c) shows that the film is single crystalline. The metal-to-insulator transition temperature, 143.9 ± 0.3 K, was obtained from a four-point resistivity measurement (see Fig. 2), as the temperature where $d\rho/dT$ changes sign. Topographs like the one in Fig. 1(d) reveal growth steps oriented along the $\mathbf{a}^*$ and $\mathbf{b}^*$ axes of the $La_{0.7}Ca_{0.3}MnO_3$ orthorhombic structure. The height of steps is systematically a multiple of c, the pseudocubic lattice parameter, indicating the same terminating layer over the whole surface. Whether it is MnO_2 or (La,Ca)O planes could not be determined because, although rugosity was on average only 1 Å, atomic resolution[24] was not achieved. As we showed in a previous paper,[25] local $I(V)$ curves are not sen-

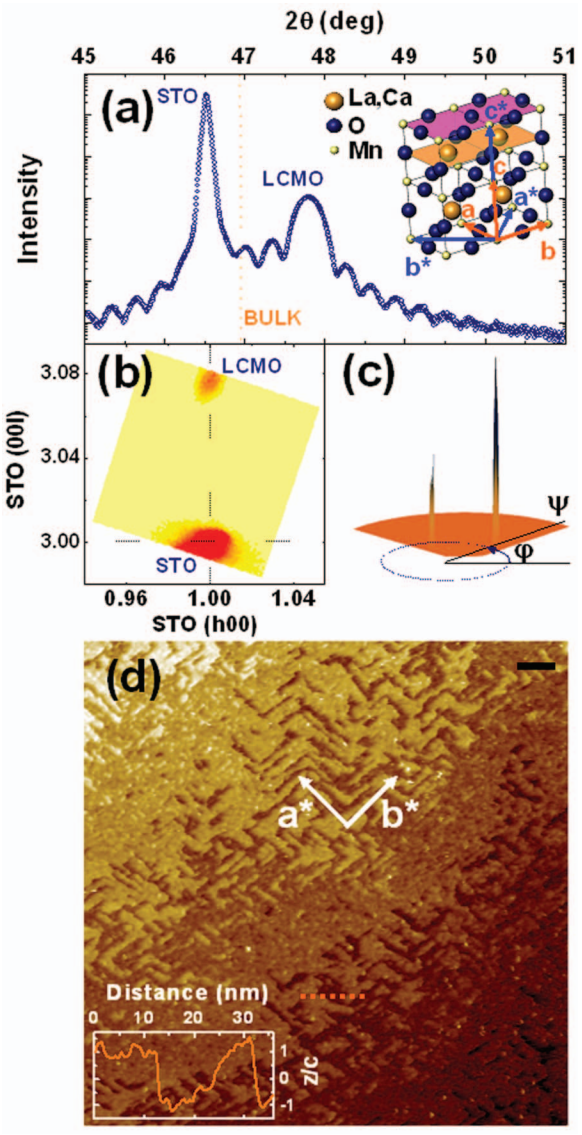

FIG. 1. (Color) (a) Main panel: X-ray diffractogram around the (002) pseudocubic reflection and size-effect oscillations. The film thickness was inferred to be 31 nm and the c axis parameter 3.808 ± 0.002 Å. Inset: Schematic crystalline structure. Pseudocubic $(\mathbf{a},\mathbf{b},\mathbf{c})$ and orthorhombic $(\mathbf{a}^*,\mathbf{b}^*,\mathbf{c}^*)$ lattice vectors are indicated, as well as MnO_2 (pink) and (La,Ca)O (orange) planes. (b) Reciprocal space map around the (103) reflection. (c) Pole-figure measurement for the (103) direction. (d) Topograph measured in the constant-current mode with regulation conditions of 2 V and 0.4 nA at 144 K. The $\mathbf{a}^*$ and $\mathbf{b}^*$ vectors of the film are at 45° to the **a** and **b** axes of the substrate. The black scale bar represents 20 nm. The height profile in the inset corresponds to the dotted line (orange).

sitive to the typical topographic features of our films and rather homogeneous at the nanoscale. Therefore the spatial average of $I(V)$ curves is representative of spectroscopic properties over the whole sample surface.

In the STS experimental configuration, where a bias voltage V is applied between the sample and the tip, the differential conductance is given by

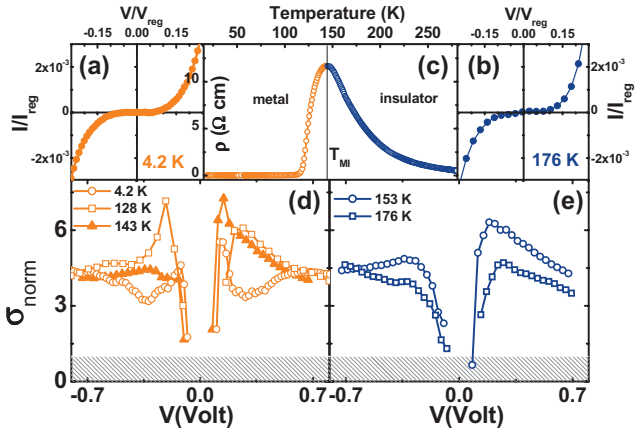

FIG. 2. (Color) Average tunneling $I(V)$ curves for (a) 4.2 K (2 V/0.5 nA) and (b) 176 K (1.3 V/0.6 nA). (c) Macroscopic resistivity data: $T_{MI}=143.9$ K is indicated by a virtual line. (d), (e) Selected normalized conductance curves at temperatures below and above T_{MI}, respectively. When the measured average current was the experimental noise ($\sim 10^{-2}$ pA) no estimation of σ_{norm} could be made (hatched regions).

$$dI/dV \approx \frac{e^2}{\hbar}\rho_s(eV)\rho_t(0)T(eV,z), \tag{1}$$

where $\rho_s(eV)$ is the sample density of states, the tip density of states $\rho_t(0)$ is assumed to be constant and z is the tip-sample separation.[26] The latter is set by the junction impedance $R_T=V_{reg}/I_{reg}$, which in STS experiments is typically 1 GΩ. If an electron is bound in a polaron, the process of an electron tunneling into the tip requires the unbinding of the quasiparticle, with an energy cost of E_b. As a consequence, STS probes the local spectrum of the quasiparticles resulting from the unbinding of polarons.

For bias voltages much smaller than the barrier height ϕ, the tunnel transmission coefficient T does not depend on V and the measured differential conductance is proportional to $\rho_s(eV)$. At voltages that are a non-negligible fraction of ϕ, as in the case of the measurements presented here, the tunnel coefficient can no longer be considered voltage independent. For moderate voltages an adequate estimation of $T(eV,z)$ is given by I/V.[26] Therefore, the numerically derived $I(V)$ curves were normalized to obtain $\sigma_{norm}=(dI/dV)/(I/V) \propto \rho_s(eV)$, the normalized conductance. At $V\sim 0$, the noise on the tunnel current hinders an appropriate estimation of $T(eV,z)$ with I/V. As a consequence, at low voltages, $T(eV,z)$ was estimated with a WKB-like tunnel transmission coefficient.[27]

In this work 10^4 single $I(V)$ curves were spatially averaged over 60×60 nm^2. Examples of average $I(V)$ curves in the metallic and insulating phases are shown in Fig. 2. At all measured temperatures dI/dV at zero bias is below the experimental resolution of typically 10^{-4} nS. In the high-temperature phase σ_{norm} presents a depletion around the Fermi level flanked by conductance peaks, as shown in Fig. 2(e). These features are the spectral signature of polarons and the half distance between the peaks, Δ_B, is a measure of the polaron binding energy.[14] The evolution of Δ_B with tempera-

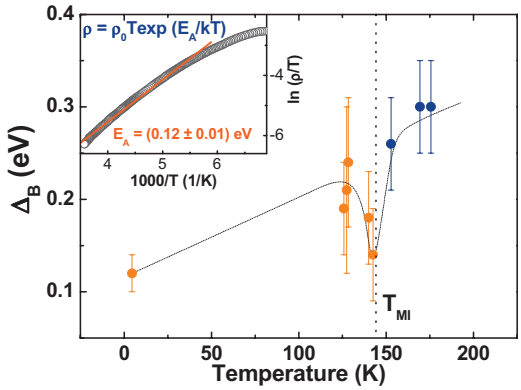

FIG. 3. (Color) Temperature dependence of the polaron binding energy estimated from normalized conductance curves as half the peak-to-peak separation (error bars stem from the uncertainty of the position of the peaks due to the voltage resolution of the spectra in Fig. 2). The solid line is a guide to the eye. Inset: Fit (red line) of the high-temperature resistivity data (open symbols) with a small-polaron adiabatic model (see text).

ture is presented in Fig. 3. At 176 K, well above T_{MI}, $\Delta_B = 0.30 \pm 0.07$ eV is consistent with the polaron binding energy obtained by fitting the high-temperature resistivity data with an adiabatic small-polaron model (see Fig. 3). Within this model $\rho = \rho_0 T \exp(E_A/kT)$ (Ref. 5) and the binding energy can be estimated as $E_b \approx 2E_A = (0.24 \pm 0.02)$ eV.[5]

In the metallic phase these polaronic characteristics persist even down to 4.2 K [see Fig. 2(d)]. Although in contrast to the theoretical prediction that polarons disappear below T_{MI},[3,4] our local spectroscopic results are consistent with data from different experimental techniques.[11–14,28] On decreasing temperature, Δ_B globally shifts to lower energies, as shown in Fig. 3. This behavior is consistent with the temperature evolution of polaron binding energies obtained from macroscopic optical reflectivity data.[28] In spite of all this evidence, the role of polarons in the transport properties of the metallic phase is currently under discussion.[29,30]

Remarkably, in addition to its global decrease with decreasing temperature, Δ_B presents a dip at T_{MI}. This dip occurs concomitantly with a sharpening of the conductance peaks for $T < T_{MI}$ [see Figs. 2(d) and 2(e)]. Whether the origin of these features can be traced to a fundamental change in the spectral properties of polarons needs to be clarified by further experimental and theoretical work. Nevertheless, the extreme sensitivity of Δ_B to the MIT and its quantitative agreement with the E_b estimated from transport data indicate that, although STS probes the quasiparticle spectrum at the surface, the σ_{norn} measured in this work is representative of bulk properties.

Normalized conductance curves in Fig. 2 come from a spatial average of 10^4 curves. The local value of the polaron binding energy can be extracted from each individual spectrum. In Figs. 4(a)–4(d) we show the polaron binding energy maps obtained upon warming from the metallic to the insulating phase in a temperature region close to T_{MI}. The maps span 60×60 nm^2 areas with a resolution of 7.5 Å (~two pseudocubic unit cells) per pixel. The spectroscopic signature of polarons is detected over the whole field of view. The

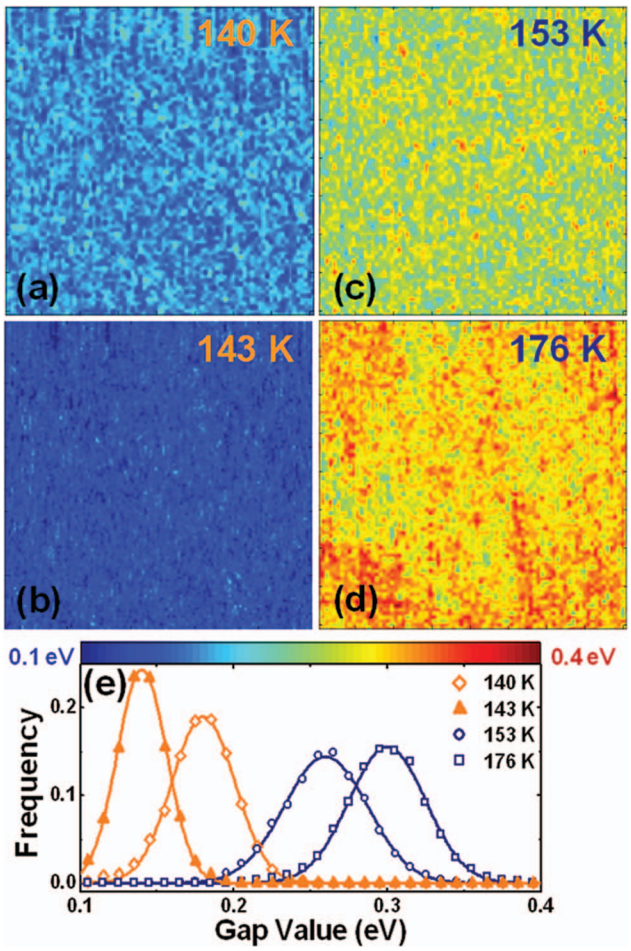

FIG. 4. (Color) Mapping of local Δ_B values at (a) 140, (b) 143, (c) 153, and (d) 176 K. All maps correspond to 60×60 nm^2 areas with a resolution of 7.5 Å/pixel. (e) Distributions of Δ_B values (symbols) obtained from the maps fitted with a Gaussian law (lines). The average noise of local $I(V)$ curves in all maps is comparable, ranging from 0.2 to 0.4 pA.

binding-energy distributions are Gaussian, as shown in Fig. 4(e). No bimodal distribution of Δ_B is detected within 0.03 eV, a resolution that is of the order of the thermal energy. The Gaussian distribution width relative to the central value does not significantly change with temperature. The results of Fig. 4 rule out a phase separation scenario where the polaronic signature in the spatially averaged spectrum would come from the averaging over coexistent polaronic and nonpolaronic regions.

At low temperatures, the nonlinear dependence of I on the bias voltage might seem in contradiction with a metallic state. This striking result can have different origins. First, in order to probe polarons, spectroscopy has to be performed in the energy scale of E_b, which is a non-negligible fraction of ϕ. As a consequence, the tip-sample separation is large and, simultaneously, the transmission coefficient increases with voltage, resulting in a nonlinear $I(V)$ characteristic. Second, the macroscopic resistivity of the 31 nm film has a value of 4 mΩ cm at 4.2 K, three orders of magnitude larger than for a common metal, implying that the number of carriers and/or their mobility is low. Recent angle-resolved photoemission

spectroscopy (ARPES) measurements in the bilayer manganite $La_{1.4}Sr_{1.6}Mn_2O_7$, revealed the presence of "nodal" quasiparticles that would account for the poor conductivity of the metallic phase.[30] Since the measured tunnel current comes from a reciprocal-space integration of the single-particle spectral function (as detected by ARPES),[31] the contribution to the tunnel conductance at E_F will be extremely small. Therefore, a low tunnel conductance at zero bias is not at odds with metallic behavior. In addition to the measurements presented in this work, previous STS studies report highly nonlinear spectra in the metallic phase of a $La_{0.7}Ca_{0.3}MnO_3$ film at 77 K,[14] and in a cleaved $La_{1.4}Sr_{1.6}Mn_2O_7$ crystal.[32] In order to study the spectral features close to the Fermi level, high energy-resolution measurements at small z are currently under way and will be the subject of a future report. We stress that this work focuses on the temperature evolution and spatial homogeneity of polaronic spectral features that are manifest at an energy scale of $\sim 0.1-1$ eV.

In summary, we present tunneling spectroscopic evidence for the presence of polarons in the insulating phase and their persistence on cooling through the insulator-to-metal transition down to 4.2 K. The spectroscopic signature of polarons is detected over the whole field of view at all measured temperatures. This novel result brings forth the challenge of understanding the role played by polaronic quasiparticles in the metallic phase of manganites.

This work was supported by the Swiss National Science Foundation and the MaNEP program of the Swiss National Center of Competence in Research.

*silvia.seiro@physics.unige.ch

[1] *Colossal Magnetoresistive Oxides*, edited by Y. Tokura, Advances in Condensed Matter Science Vol. 2 (Gordon and Breach, Amsterdam, 2000).

[2] E. Dagotto, *Nanoscale Phase Separation and Colossal Magnetoresistance* (Springer-Verlag, Berlin, 2003).

[3] A. J. Millis, P. B. Littlewood, and B. I. Shraiman, Phys. Rev. Lett. **74**, 5144 (1995).

[4] A. J. Millis, B. I. Shraiman, and R. Mueller, Phys. Rev. Lett. **77**, 175 (1996).

[5] D. C. Worledge, G. J. Snyder, M. R. Beasley, T. H. Geballe, R. Hiskes, and S. DiCarolis, J. Appl. Phys. **80**, 5158 (1996).

[6] M. Jaime, M. B. Salamon, M. Rubinstein, R. E. Treece, J. S. Horwitz, and D. B. Chrisey, Phys. Rev. B **54**, 11914 (1996).

[7] J. M. De Teresa, M. R. Ibarra, P. A. Algarabel, C. Ritter, C. Marquina, J. Blasco, J. García, A. del Moral, and Z. Arnold, Nature (London) **386**, 256 (1997).

[8] M. Quijada, J. Černe, J. R. Simpson, H. D. Drew, K. H. Ahn, A. J. Millis, R. Shreekala, R. Ramesh, M. Rajeswari, and T. Venkatesan, Phys. Rev. B **58**, 16093 (1998).

[9] P. Dai, J. A. Fernandez-Baca, N. Wakabayashi, E. W. Plummer, Y. Tomioka, and Y. Tokura, Phys. Rev. Lett. **85**, 2553 (2000).

[10] S. H. Chun, M. B. Salamon, Y. Tomioka, and Y. Tokura, Phys. Rev. B **61**, R9225 (2000).

[11] M. F. Hundley, M. Hawley, R. H. Heffner, Q. X. Jia, J. J. Neumeier, J. Tesmer, J. D. Thompson, and X. D. Wu, Appl. Phys. Lett. **67**, 860 (1995).

[12] A. S. Alexandrov, G.-M. Zhao, H. Keller, B. Lorenz, Y. S. Wang, and C. W. Chu, Phys. Rev. B **64**, 140404(R) (2001).

[13] G.-M. Zhao, V. Smolyaninova, W. Prellier, and H. Keller, Phys. Rev. Lett. **84**, 6086 (2000).

[14] J. Y. T. Wei, N. C. Yeh, and R. P. Vasquez, Phys. Rev. Lett. **79**, 5150 (1997).

[15] K. H. Kim, J. H. Jung, and T. W. Noh, Phys. Rev. Lett. **81**, 1517 (1998).

[16] A. Lanzara, N. L. Saini, M. Brunelli, F. Natali, A. Bianconi, P. G. Radaelli, and S.-W. Cheong, Phys. Rev. Lett. **81**, 878 (1998).

[17] M. Fäth, S. Freisem, A. A. Menovsky, Y. Tomioka, J. Aarts, and J. A. Mydosh, Science **285**, 1540 (1999); sample characterization is described in S. Freisem, A. Brockhoff, D. G. de Groot, B. Dam, and J. Aarts, J. Magn. Magn. Mater. **165**, 380 (1997).

[18] T. Becker, C. Streng, Y. Luo, V. Moshnyaga, B. Damaschke, N. Shannon, and K. Samwer, Phys. Rev. Lett. **89**, 237203 (2002).

[19] S. F. Chen, P. I. Lin, J. Y. Juang, T. M. Uen, K. H. Wu, Y. S. Gou, and J. Y. Lin, Appl. Phys. Lett. **82**, 1242 (2003).

[20] V. Moshnyaga, L. Sudheendra, O. I. Lebedev, S. A. Köster, K. Gehrke, O. Shapoval, A. Belenchuk, B. Damaschke, G. van Tendeloo, and K. Samwer, Phys. Rev. Lett. **97**, 107205 (2006).

[21] J. Mitra, M. Paranjape, A. K. Raychaudhuri, N. D. Mathur, and M. G. Blamire, Phys. Rev. B **71**, 094426 (2005).

[22] X. F. Song, G. J. Lian, and G. C. Xiong, Phys. Rev. B **71**, 214427 (2005); S. Seiro, E. Koller, Y. Fasano, and Ø. Fischer, Appl. Phys. Lett. **91**, 091913 (2007).

[23] A. D. Kent, Ch. Renner, Ph. Niedermann, J.-G. Bosch, and Ø. Fischer, Ultramicroscopy **42-44**, 1632 (1992).

[24] To our knowledge, atomic resolution on manganite films has only been recently achieved and reported in J. X. Ma, D. T. Gillaspie, E. W. Plummer, and J. Shen, Phys. Rev. Lett. **95**, 237210 (2005).

[25] S. Seiro, Y. Fasano, I. Maggio-Aprile, O. Kuffer, and Ø. Fischer, J. Magn. Magn. Mater. **310**, 243 (2006).

[26] P. Mårtensson and R. M. Feenstra, Phys. Rev. B **39**, 7744 (1989).

[27] V. A. Ukraintsev, Phys. Rev. B **53**, 11176 (1996).

[28] C. Hartinger, F. Mayr, J. Deisenhofer, A. Loidl, and T. Kopp, Phys. Rev. B **69**, 100403(R) (2004).

[29] Guo-meng Zhao, H. Keller and W. Prellier, J. Phys.: Condens. Matter **12**, L361 (2000).

[30] N. Mannella, W. L. Yang, X. J. Zhou, H. Zheng, J. F. Mitchell, J. Zaanen, T. P. Devereaux, N. Nagaosa, Z. Hussain, and Z.-X. Shen, Nature (London) **438**, 474 (2005).

[31] Ø. Fischer, M. Kugler, I. Maggio-Aprile, C. Berthod, and Ch. Renner, Rev. Mod. Phys. **79**, 353 (2007).

[32] H. M. Rønnow, Ch. Renner, G. Aeppli, T. Kimura, and Y. Tokura, Nature (London) **440**, 1025 (2006).